Solar Energy Materials & Solar Cells 131 (2014) 92–99

Contents lists available at ScienceDirect

Solar Energy Materials & Solar Cells

journal homepage: www.elsevier.com/locate/solmat

Towards a unified low-field model for carrier mobilities in crystalline silicon

Florian Schindler [a,b,*], Maxime Forster [c], Juliane Broisch [a], Jonas Schön [a], Johannes Giesecke [a], Stefan Rein [a], Wilhelm Warta [a], Martin C. Schubert [a]

[a] Fraunhofer Institut für Solare Energiesysteme, Heidenhofstraße 2, 79110 Freiburg, Germany
[b] Freiburger Materialforschungszentrum, Albert-Ludwigs-Universität Freiburg, Stefan-Meier-Straße 21, 79104 Freiburg, Germany
[c] Apollon Solar, 66, Cours Charlemagne, 69002 Lyon, France

ARTICLE INFO

Available online 19 June 2014

Keywords:
Mobility
Compensation
Silicon
Phonon scattering

ABSTRACT

The electrical properties of crystalline silicon crucially depend on the mobility of minority and majority charge carriers. As parameters like the conductivity and the diffusion length are directly connected to carrier mobility, its exact prediction is essential for device simulation and material characterization. While generally accepted mobility models exist for uncompensated silicon, strong deviations have been observed in compensated silicon depending on the compensation level. Different approaches have been suggested for modeling majority carrier mobility correcting for compensation. In this work, the controversially discussed physical reasons for mobility reductions in compensated silicon are critically reviewed and we present a unified description of mobility in silicon. Based on the approach suggested by Schindler et al. [Solar Energy Materials and Solar Cells 106 (2012) 31–36], which describes the modeling of majority carrier mobilities in p-type compensated silicon at room temperature, the model is extended to both majority and minority carrier mobilities in p- and n-type compensated silicon at room temperature and a description for the temperature dependence is suggested. Fit parameters are obtained based on a wide range of published and new carrier mobility data presented here. Additionally, a new parameterization for scattering of holes by phonons is presented and included in the model.

1. Introduction

Although accounting for the simultaneous presence of acceptors and donors as scattering centers, Klaassen's mobility model [1] fails to correctly describe carrier mobilities in compensated silicon [2–12]. As Klaassen's model is based on the empirical mobility expression of Caughey and Thomas [13] developed for uncompensated silicon, and parameters are obtained from fitting experimental data in uncompensated silicon, not quite unexpected deviations are found for compensated silicon. It has been shown in several publications, e.g. [10,11], that the deviation from Klaassen's model depends on the compensation level. In a previous work [10], reduced mobilities are explained by reduced screening which is not sufficiently taken into account in Klaassen's model. This assumption is challenged by temperature dependent measurements in other publications [8,11], suggesting that reduced screening alone cannot explain mobility reductions along the whole temperature range.

In this work we show that temperature dependent measurements do not necessarily contradict the hypothesis of reduced screening as a reason for mobility reductions. The approach suggested in [10] is used as a starting point for a unified description of mobilities in compensated silicon. We first show that a single set of parameters can be used for the description of both majority hole and electron carrier mobility in compensated silicon at room temperature. Using the same parameter set and introducing an additional dependence on the total dopant concentration also allows for modeling minority electron and hole mobility. In a third step, the model is extended to correctly describe mobility data in compensated silicon along the temperature range from 80 to 350 K including a new phenomenological parameterization for hole scattering at phonons. Thus, a unified mobility model is obtained, which merges with Klaassen's mobility model including

* Corresponding author at: Fraunhofer Institut für Solare Energiesysteme, Heidenhofstraße 2, 79110 Freiburg, Germany. Tel.: +49 761 4588 5321; fax: +49 761 4588 9250.
E-mail addresses: florian.schindler@ise.fraunhofer.de (F. Schindler), forster@apollonsolar.com (M. Forster), juliane.broisch@ise.fraunhofer.de (J. Broisch), jonas.schoen@ise.fraunhofer.de (J. Schön), johannes.giesecke@ise.fraunhofer.de (J. Giesecke), stefan.rein@ise.fraunhofer.de (S. Rein), wilhelm.warta@ise.fraunhofer.de (W. Warta), martin.schubert@ise.fraunhofer.de (M.C. Schubert).

http://dx.doi.org/10.1016/j.solmat.2014.05.047
0927-0248/

a new parameterization for hole scattering at phonons in the case of uncompensated silicon.

2. Physical motivation and approach

In order to motivate the approach presented in this work, some remarks are required regarding the origin of mobility reductions in compensated silicon. Mobility reductions in compensated silicon have been frequently observed in the past years [2–12]. The reasons were controversially discussed and different approaches to account for these mobility reductions were suggested. In [6], a mobility correction term $\mu_{cor} \propto C_l^{-3/4}$, C_l denoting the compensation level, attributed to a specific compensation effect which is not taken into account in the existing mobility models is suggested. Adding such a correction term according to Matthiesen's rule ($1/\mu = 1/\mu_{Klaassen} + 1/\mu_{cor}$) can only be justified with an additional scattering channel in compensated silicon, which has not been proven to exist so far. In [9] it is argued that the discrepancy of experimental and modeled mobility values in compensated silicon highlights the non-physical character of Klaassen's model rather than a mobility reduction due to compensation as Klaassen's model is based on a substantial amount of fitting to data in uncompensated silicon. A correct mobility description would therefore require a complete re-assessment of Klaassen's fitting parameters. Alternatively, a very simple empirical correction for compensation is suggested in that work: by multiplying Klaassen's mobility with a prefactor depending on the compensation level and the type of carrier, a good description of mobility in compensated silicon can be achieved. While the simplicity is the strength of this correction, its weakness is its purely empirical nature.

An approach previously put forward by some of the authors attempted to stay as close as possible to the largely successful Klaassen's model [10]. As an explanation for reduced mobilities in compensated silicon a reduction of screening that is not accounted for sufficiently in Klaassen's model was introduced. By adding a compensation-dependent term accounting for reduced screening in the Caughey–Thomas mobility expression, which is the empirical starting point in Klaassen's model, we tried to keep the physical character of the model. However, temperature dependent measurements appeared to contradict this hypothesis, as reducing the temperature increases the compensation level without a further strong mobility reduction [8]. A closer look at the implementation of the T-dependence of impurity scattering in Klaassen's model [14] allows for solving this apparent contradiction

$$\mu_{i,l} = \frac{\mu_{max}^2}{\mu_{max} - \mu_{min}} \left(\frac{N_{ref,1}}{N_I}\right)^{\alpha_1} \left(\frac{T}{300\ \mathrm{K}}\right)^{3\alpha_1 - 1.5} + \frac{\mu_{min} \cdot \mu_{max}}{\mu_{max} - \mu_{min}} \left(\frac{c}{N_I}\right) \left(\frac{300\ \mathrm{K}}{T}\right)^{0.5} \quad (1)$$

The second term in this equation accounts for reduced screening with decreasing carrier concentration c at a constant concentration of ionized scattering centers N_I. As argued in [10], at room temperature the first term is predominant for dopant concentrations $N \leq N_{ref} = 2.23 \times 10^{17}\ \mathrm{cm}^{-3}$, i.e. reduced screening is not taken into account adequately in Klaassen's model in this dopant range. With decreasing temperature, however, the second term becomes more important (e.g. at 100 K, the first term is reduced to 50% of its room-T value, while the second term is roughly doubled). This means, the lower the temperature, the more Klaassen's model already accounts for reduced screening in compensated silicon without any correction. Therefore, comparing mobilities with Klaassen's model for the case of an increased compensation level by doping at room temperature and for the case of increased compensation level by a temperature reduction is actually expected to lead to a completely different behavior. Consequently, temperature dependent mobility measurements in compensated silicon are not necessarily in contradiction with the assumption of reduced screening as a reason for reduced mobilities at room temperature. Therefore, in this work we follow the approach presented in [10] to install a mobility model predicting mobilities in uncompensated and compensated silicon. Our reasoning to put this approach forward is that the introduction of the compensation-dependent correction term in the empirical Caughey–Thomas expression can at least be physically motivated.

In the first part we will extend the model presented for majority hole mobilities in compensated p-type silicon [10] to majority and minority hole and electron mobilities in compensated p- and n-type silicon and obtain the fit parameters from a larger data base including new mobility data in compensated silicon. In the second part we will discuss the temperature dependence of majority carrier mobilities in compensated silicon from 80 to 350 K including a new parameterization of the phonon-scattering. Details on the model implementation are summarized in Appendix C.

3. Results

3.1. Modeling mobility at room temperature

3.1.1. Majority hole and electron mobility

In this section we present new majority hole and electron mobility data in compensated p- and n-type silicon, obtained from Hall measurements on different materials at two different institutes. Details on the measurement techniques at Fraunhofer ISE can be found in [15], details on the measurement techniques used by Apollon Solar in [8]. Dopant concentrations and measured mobilities which have not been published so far are listed in Appendix A. Fig. 1a presents the data (colored symbols) plotted as relative deviation from Klaassen's model as a function of the compensation level $C_l = (N_A + N_D)/c$, where $N_A + N_D$ is the sum of ionized acceptors and donors and c the free carrier concentration $n_0 + p_0$. Note that all data presented in this work was obtained from experiments without injection of carriers for majority carrier measurements and under low injection of carriers for minority carrier measurements. Additionally we include data from reference [11], which were not considered yet by the model fit done in [10].

These new data follow the same trend as the earlier published data (plotted as gray crosses) collected in [10], and, remarkably, relative deviations from Klaassen's model are the same for majority hole and majority electron mobility, measured on compensated p-type and n-type silicon respectively. Following the approach presented in [10], we use a modified Caughey–Thomas mobility expression

$$\mu = \frac{\mu_{max} - \mu_{min}}{1 + (N/N_{ref})^{\alpha} + ((C_l - 1)/C_{l,ref})^{\beta_1}} + \mu_{min} \quad (2)$$

as a starting point for Klaassen's model. Details on the implementation can be found in [10] and in Appendix C. The fit parameters $C_{l,ref}$ and β are adjusted for the majority hole and electron mobilities by additionally taking these new mobility data into account

$$C_{l,\,ref} = 24.82 \pm 2; \quad \beta_1 = 1.092 \pm 0.03 \quad (3)$$

Note that mobility data from [4], which had been considered in the fitting in [10], is neglected in this work. In [4], compensation was achieved by activation of thermal donors, thereby introducing doubly ionized scattering centers. When plotted as a function of the compensation level, these mobility data show a significantly larger spread than mobility data from compensated material solely containing singly charged scattering centers. The larger spread can be due to several reasons. On the one hand, the scattering power

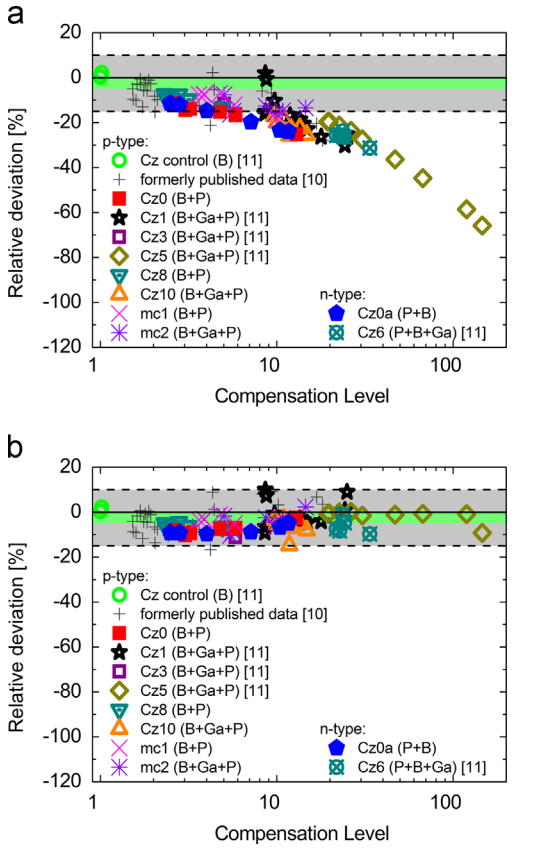

Fig. 1. Relative deviation of majority hole and electron mobility measured in compensated p- and n-type silicon from Klaassen's model (a) and from the corrected model presented here (b). The accepted tolerance due to differences between mobility measurements of uncompensated multi- and monocrystalline silicon is marked in green, the typical uncertainty range of mobility measurements is marked in gray. (For interpretation of the references to color in this figure legend, the reader is referred to the web version of this article.)

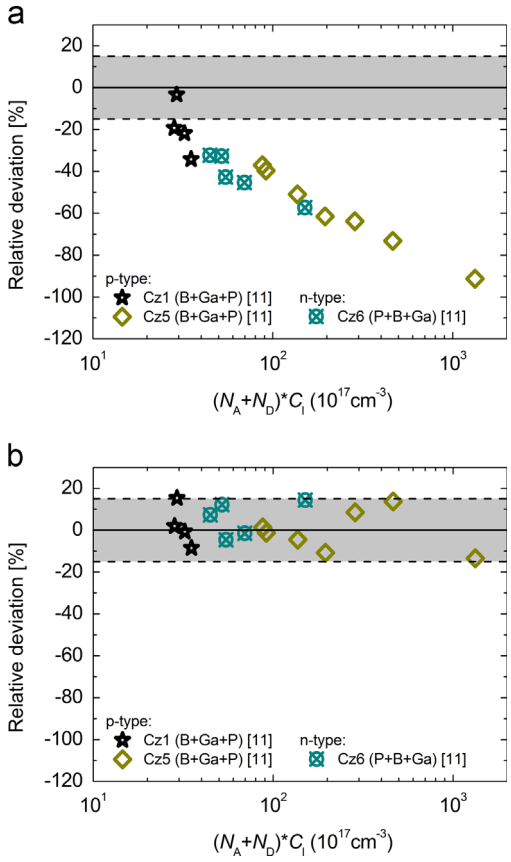

Fig. 2. Deviation of minority electron and hole mobility measured in compensated silicon from Klaassen's model (a) and from the corrected model presented in this work (b).

of a doubly ionized scattering center is enhanced by a factor of four compared to a singly charged impurity, thereby changing the ratio of the concentration of donors and their scattering power, which also sensitively influences the definition of the compensation level. Additionally, as discussed in [12], heterogeneities in the doping concentrations are observed across samples compensated by thermal donor activation, even leading to the formation of a n–p–n transistor for high compensation levels arising from the preferential formation of thermal donors in the sample's subsurface. This would have a significant impact on the mobility obtained from Hall measurements and would lead to large uncertainties when plotting the mobility data as a function of compensation level. To keep the uncertainties to a minimum, for the model fit we only consider mobility data from samples compensated by singly ionized dopants. This data is shown in Fig. 1. As shown in [16], a mobility reduction of about 5% can already occur in uncompensated multicrystalline silicon. As this reduction is not attributed to compensation, data with a maximum reduction of 5% was treated as correct mobility data. Therefore, in the fit χ^2 was reduced by only accounting for positive deviations or negative deviations larger than 5%. Thus, excellent agreement between the model and the experimental data is obtained (cf. Fig. 1b), both for majority hole mobilities in compensated p-type silicon and majority electron mobilities in compensated n-type silicon, with maximum relative deviations of $+10\%$ and -15%, which are in the range of estimated uncertainties of mobility measurements. Note that this error comprises both errors of the measured mobility itself as well as errors of the modeled mobility due to uncertainties of dopant and carrier concentrations, which are the input parameters for the modeled mobility.

3.1.2. Minority hole and electron mobility

A significant reduction compared to Klaassen's model is also observed for minority carrier mobilities in compensated p- and n-type silicon [11]. By applying the model developed for majority carrier mobilities from Section 3.1.1, the deviation is decreased, but a pronounced dependence on compensation level remains. Even a new fit of the parameters $C_{l,ref}$ and β_1 based on the data for minority carrier mobilities does not lead to a good description of the experimental data. This indicates that the deviation is not only a function of the compensation level. We observe that this deviation is additionally a function of the total ionized dopant concentration (N_A+N_D), which is illustrated in Fig. 2a where the relative deviation of minority electron and hole mobility [11] from Klaassen's model is plotted as a function of $(N_A+N_D)\cdot C_l$. Thus, this observation may be accounted for by weighting the correction term in Eq. (2) obtained for majority carriers accordingly, leading to the expression

$$\left(\left[\frac{N_A+N_D}{N_{ref,3}}\right]\cdot\left[\frac{C_l-1}{C_{l,ref}}\right]\right)^{\beta_1} \tag{4}$$

By inserting one new parameter, $N_{ref,3}=(1.276\pm0.1)\times 10^{17}\,\mathrm{cm}^{-3}$, while leaving $C_{l,ref}$ and β_1 unchanged, the same correction can be applied for minority carrier mobilities. Results are shown in Fig. 2b.

This additional term weights the compensation level with the total ionized dopant concentration. As the definition of the compensation level is a priori arbitrary, one could also regard this

term as a redefinition of the compensation level emphasizing the ionized dopant concentration in a more pronounced way than the free carrier concentration. This means that with increasing compensation the minority carrier mobility reacts more sensitively to an increase in the total dopant concentration than the majority carrier mobility. In other words, for a constant total dopant concentration and an increasing compensation level, the minority carrier mobility reacts less sensitively to a decrease in the free carrier concentration n_0+p_0 than the majority carrier mobility. This shall be tentatively explained in the following. Klaassen's model accounts for the attractive interaction potential for free carrier scattering. Due to the higher concentration of majority carriers acting as scattering centers for minority carriers, this term is much more important for minority carriers. Furthermore, for the minority carrier mobility in uncompensated silicon scattering at carriers is even more important than scattering at majority impurities. This is due to the larger scattering potential of attractive free carriers compared to repulsive stationary scattering centers as explained in [1]. Therefore, tuning the compensation level has a different impact on minority and majority carriers: when compensation is increased by solely decreasing the free carrier concentration while leaving the total dopant concentration constant, the majority carrier mobility is reduced due to reduced screening of the impurity scattering potential. The minority carrier mobility is also affected by the reduced screening of the impurity scattering potential, but at the same time, scattering at free majority carriers is reduced. Consequently, increasing the compensation level by increasing the total dopant concentration reduces the minority carrier mobility more strongly than increasing the compensation level by reducing the free majority carrier concentration. This can be accounted for in the model by weighting the compensation correction term with the total dopant concentration according to Eq. (4). More experimental data for minority carrier mobilities in compensated silicon would be useful to strengthen this hypothesis.

The model implementation is explained in more detail in Appendix C.

3.2. Modeling mobility in the temperature range from 80 to 350 K

3.2.1. Phonon scattering

Before discussing the effect of compensation on mobilities over the temperature range 80–350 K, we will first focus on the phonon scattering. As observed in [12], Klaassen's model seems to overestimate the phonon scattering of holes in the range from 80 to 300 K. This is in agreement with previous publications [17,18]. Szmulowicz numerically calculates acoustic and optical-phonon-limited mobilities in p-type silicon within the deformation-potential theory [17]. Although such an approach would be the most physical description of phonon scattering, analytical expressions are needed for device simulations. Klaassen's model uses a simple power law for the temperature dependence of phonon scattering of holes

$$\mu_{phonons,\ Klaassen} = 470.5\,\frac{\mathrm{cm}^2}{\mathrm{Vs}}\cdot\left(\frac{300\ \mathrm{K}}{T}\right)^{2.247} \tag{5}$$

However, this parameterization underestimates Szmulowicz's mobility values in the temperature range from 50 to 300 K. Mobilities recently measured by Veirman et al. in ultra-pure lowly doped 5000 Ω cm p-type silicon support this underestimation of $\mu_{phonons}$ by Klaassen's model [12]. They suggested to account for this deviation by using an alternative parameterization for the phonon scattering instead

$$\mu_{phonons,Veirman} = \exp(aT^6+bT^5+cT^4+dT^3+eT^2+fT+g) \tag{6}$$

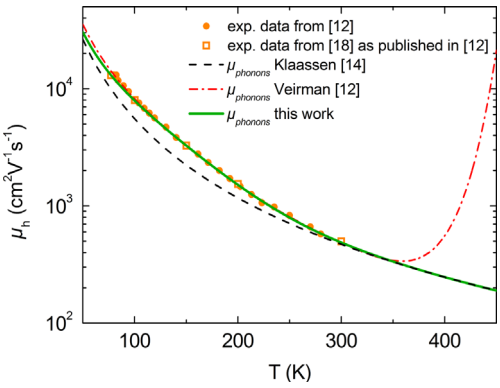

Fig. 3. Comparison of the three parameterizations for the temperature dependence of phonon scattering of holes suggested by Klaassen [14], Veirman et al. [12] and in this work with experimental data published in [12,18].

with the seven parameters *a*–*g* published in [12]. Veirman's parameterization reproduces the experimental data and Szmulowicz's model for temperatures between 80 K and 300 K. However, due to its polynomial character it is stable only in a certain temperature interval and behaves unphysically at temperatures higher than 350 K (see Fig. 3). This will lead to significant errors when using this parameterization at higher temperatures. Therefore, a new parameterization for phonon scattering is needed which behaves physically meaningful in the whole temperature range. We used Klaassen's parameterization for hole scattering at phonons as a starting point and, also empirically, added an exponential function to account for the deviation in the temperature range between 80 K and 300 K

$$\mu_{phonons} = 470.5\,\frac{\mathrm{cm}^2}{\mathrm{Vs}}\cdot\left(\frac{300\ \mathrm{K}}{T}\right)^{2.247} + \mu_{corr}\cdot\exp\left(-\left(\frac{T}{T_{corr}}\right)^{\theta_{h,corr}}\right) \tag{7}$$

A fit to the data published in [12], which also includes data from [18], delivers the parameters $\mu_{corr} = 4800\ \mathrm{cm}^2\ \mathrm{V}^{-1}\ \mathrm{s}^{-1}$, $T_{corr} = 120$ K and $\theta_{h,corr} = 1.9$. Excellent agreement with the data is achieved (cf. Fig. 3). Compared to the parameterization suggested in [12], our parameterization features the following advantages: it behaves physically meaningful in the whole temperature range and merges with Klaassen's parameterization at high and low temperatures, thus it is able to exclusively account for the deviation in the temperature range covered by experimental data. In particular, it does not diverge for temperatures above 350 K and can therefore be used for device simulation in the whole temperature range. Furthermore, this new parameterization introduces only three new parameters compared to seven in the parameterization suggested in [12].

3.2.2. Temperature dependence of mobility in compensated silicon

Due to incomplete ionization at low temperatures [8], phonon scattering is important in the entire temperature range in uncompensated silicon. In compensated silicon incomplete ionization is less pronounced, as the total density of ionized dopants cannot decrease below $2\times[N_{dop,min}]$, where $[N_{dop,min}]$ denotes the minority dopant concentration [8]. As a consequence, in compensated silicon ionized impurity scattering becomes more important with decreasing temperature than in uncompensated silicon. However, a good description of the temperature dependence of mobilities in compensated silicon is still lacking [9,12].

In this section we will discuss the temperature dependence of majority carrier mobility in compensated silicon. Fig. 4 shows mobility data obtained from Hall measurements and recalculated with the temperature dependent Hall factor from reference [19] in a compensated p-type sample featuring a compensation level of

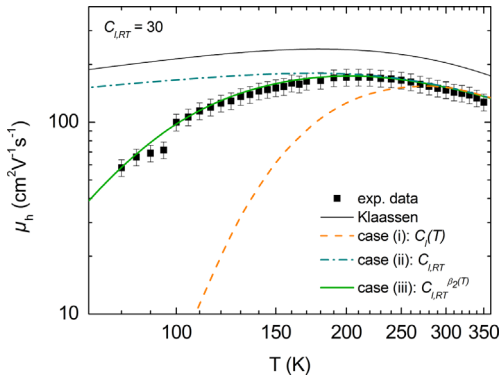

Fig. 4. Hole mobility in a compensated p-type sample obtained from Hall measurements compared to Klaassen's model and three variations of the model presented in this work.

30, an acceptor concentration of $2.80\times10^{17}\,\mathrm{cm}^{-3}$ and a donor concentration of $2.62\times10^{17}\,\mathrm{cm}^{-3}$ at room temperature. Measurements were conducted in the frame of Maxime Forster's Ph.D. thesis [9]. We compare the experimental data to Klaassen's model and to three variations of the model which are summarized below. For the model presented here we always use the phonon scattering of Eq. (7).

In order to leave the compensation-dependent correction term introduced for room temperature in Section 3.1.1 unaffected by the temperature dependence of Klaassen's model, we account for the temperature dependence in the impurity scattering term before introducing the compensation-dependent term, leading to the following expression for impurity scattering:

$$\mu_I=\frac{\mu_N}{((N_I)/(N_{ref,1}))^{\alpha_1}/((T)/(300\ \mathrm{K}))^{3\alpha_1-1.5}+\left((C_l(T)-1)/(C_{l,ref})\right)^{\beta_1}}+\mu_c\left(\frac{c}{N_I}\right)\left(\frac{300\ \mathrm{K}}{T}\right)^{0.5} \tag{8}$$

$C_l(T)$ is the compensation level at the corresponding temperature T. As the free carrier concentration strongly decreases with decreasing temperature, the compensation level strongly increases. Using this temperature dependent compensation level in the correction term leads to a large underestimation of mobilities by the model. This is depicted by case (i) in Fig. 4. To illustrate the correction using a temperature independent compensation level as input, we also plotted the modeled mobility using the following expression for impurity scattering:

$$\mu_I=\frac{\mu_N}{((N_I)/(N_{ref,1}))^{\alpha_1}/((T)/(300\ \mathrm{K}))^{3\alpha_1-1.5}+((C_{l,RT}-1)/(C_{l,ref}))^{\beta_1}}+\mu_c\left(\frac{c}{N_I}\right)\left(\frac{300\ \mathrm{K}}{T}\right)^{0.5} \tag{9}$$

$C_{l,RT}$ denotes the compensation level at room temperature which in case (ii) is used for modeling mobilities along the whole temperature range. As shown in Fig. 4, this leads to an overestimation of mobilities at low temperatures. This is not surprising, as the compensation level increases with decreasing temperature, which is not accounted for in case (ii). However, as shown in case (i), taking into account the actual compensation level at each temperature leads to a strong underestimation of mobilities at low temperatures. This seeming contradiction can be explained as outlined in Section 2: adjusting the compensation level by changing the temperature leads to a different behavior than adjusting the compensation level just by doping. Hence, the compensation term introduced for the room temperature correction of mobilities is not necessarily directly transferable to the whole temperature range.

As compensation indeed depends on the temperature, but using the actual compensation level at each temperature overemphasizes the correction term at low temperatures, we start with the room temperature compensation level and implement an empirical temperature dependence accounting for the increasing compensation level with decreasing temperature. As the compensation correction at 300 K is also an empirical correction, it is justified to introduce a further empirical correction in this term to account for the temperature dependence. This can be done with the following expression for impurity scattering:

$$\mu_I=\frac{\mu_N}{((N_I)/(N_{ref,1}))^{\alpha_1}/((T)/(300\ \mathrm{K}))^{3\alpha_1-1.5}+((C_{l,RT}{}^{\beta_2(T)}-1)/(C_{l,ref}))^{\beta_1}}+\mu_c\left(\frac{c}{N_I}\right)\left(\frac{300\ \mathrm{K}}{T}\right)^{0.5} \tag{10}$$

$C_{l,RT}$ is the room temperature compensation level and $\beta_2(T)$ is a temperature dependent term accounting for an increasing compensation level with decreasing temperature

$$\beta_2(T)=1+\frac{60}{\sqrt{C_{l,RT}}}\exp\left(-\left(\frac{T}{T_{ref}}+1.18\right)^2\right) \tag{11}$$

where T_{ref} denotes a reference temperature depending on the room temperature compensation level and the total dopant concentration

$$T_{ref}=37.9\ \mathrm{K}\cdot\ln\left(\frac{C_{l,RT}{}^2\cdot(N_A+N_D)}{10^{19}\ \mathrm{cm}^{-3}}+3.6\right) \tag{12}$$

The derivation of $\beta_2(T)$ is explained in detail in Appendix B. Using $C_{l,RT}{}^{\beta_2(T)}$ in the correction term leads to case (iii) in Fig. 4.

As explained in more detail in Appendix B, $\beta_2(T)$ was adjusted to correctly describe the temperature dependence of the majority carrier mobility of a large set of about 30 samples stemming from three different compensated p-type ingots and one compensated n-type ingot covering a wide range of compensation levels ($C_{l,RT}=5-145$) as well as dopant concentrations, net doping concentrations and resistivities ($N_A+N_D=(1-9)\times10^{17}\,\mathrm{cm}^{-3}$; $p_0\,(300\ \mathrm{K})=(0.6-7)\times10^{16}\,\mathrm{cm}^{-3}$; $\rho\,(300\ \mathrm{K})=(0.5-19)\,\Omega\,\mathrm{cm}$). Therefore, the description of the temperature dependence of mobility in compensated silicon over the temperature range 80–350 K is experimentally validated in this range of compensation levels and doping concentrations, which gives confidence that it is valid for compensated silicon in general. For the sake of clarity, not all temperature dependent data can be shown in this paper. Fig. 5 exemplarily shows the experimental data of five compensated p-type samples and two compensated n-type samples with room temperature compensation levels covering a range from 15 to 145. Room temperature values of ionized dopant concentrations and compensation levels are listed in Table 1. Excellent agreement between data and the model presented here (Eq. (10)) is obtained for all temperatures and compensation levels with the same set of fitting parameters.

The data plotted in Fig. 5 is a representative selection of seven of about 30 samples investigated in this work. Agreement between measured mobility and model for all other samples not shown in the graph is of similar quality. Measurements were conducted in the frame of Maxime Forster's Ph.D. thesis [9] and partly published in [8,9,11]. Details on the measurement techniques and the calculation of the ionized dopant concentrations including incomplete ionization can also be found in these publications.

Details on implementing the corrections in Klaassen's model and a discussion about a preliminary description of the temperature dependence of the minority carrier mobility in compensated silicon can be found in Appendix C.

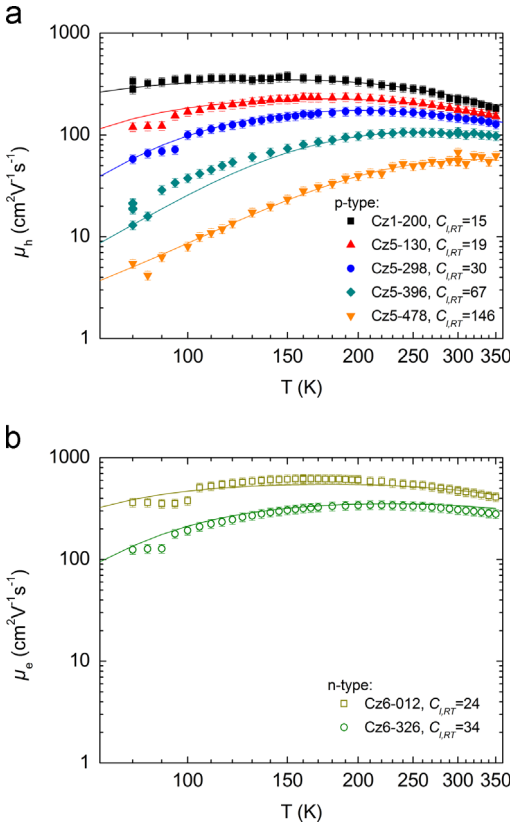

Fig. 5. Experimental T-dependent majority carrier mobility of (a) five compensated p-type and (b) two compensated n-type samples with a wide range of compensation levels compared to the model presented here (lines).

Table 1
Ionized dopant concentrations and compensation level at 300 K for the samples shown in Fig. 5.

Sample	Type	N_A (cm^{-3})	N_D (cm^{-3})	$C_{l,RT}$
Cz6-012	n	9.20×10^{16}	1.00×10^{17}	24
Cz6-326	n	2.02×10^{17}	2.14×10^{17}	34
Cz1-200	p	9.83×10^{16}	8.60×10^{16}	15
Cz5-130	p	2.32×10^{17}	2.09×10^{17}	19
Cz5-298	p	2.80×10^{17}	2.62×10^{17}	30
Cz5-396	p	3.37×10^{17}	3.27×10^{17}	67
Cz5-478	p	4.34×10^{17}	4.28×10^{17}	146

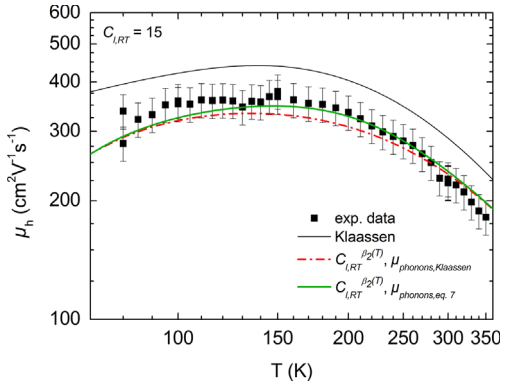

Fig. 6. Experimental hole mobility in a compensated p-type sample compared to Klaassen's model and the model presented in this work including or not the new parameterization for phonon scattering. (For interpretation of the references to color in this figure, the reader is referred to the web version of this article.)

Finally, we want to demonstrate the benefit of the new parameterization for phonon scattering for the case of compensated silicon. Fig. 6 shows exemplarily the temperature dependence of the hole mobility in the compensated p-type sample Cz1-200 listed in Table 1. We compare the experimental data to Klaassen's model, which overestimates the mobility in the whole temperature range. The comparison of the data with the model suggested in this work shows, that including the parameterization of phonon scattering from Eq. (7) significantly better describes the data in the temperature range from 100 to 300 K (green line) than the same model including Klaassen's parameterization of phonon scattering (red dashed line). Note that for this sample, the temperature correction $\beta_2(T)$ significantly influences the modeled mobility only below 120 K. This demonstrates again the accurate description of phonon scattering by the parameterization suggested in this work.

Furthermore, the mobility results of the n-type samples shown in Fig. 5b suggest that also for electron scattering at phonons a new parameterization would be helpful, as the curvature of the data is larger than the curvature of the modeled values. Therefore, temperature dependent data on high purity and high resistivity n-type silicon would be needed to transfer the approach presented in this work to electron phonon scattering.

4. Conclusions

Comparing experimental carrier mobility data in crystalline silicon with Klaassen's mobility model demonstrates that majority and minority carrier mobilities in compensated p- and n-type silicon are overestimated by the model. Additionally, the hole scattering at phonon seems to be overestimated by Klaassen's model in the temperature range from 80 to 300 K.

Based on the approach presented in [10], where mobility reductions in compensated silicon are attributed to reduced screening not accounted for sufficiently in Klaassen's model, we extend the compensation correction introduced for majority hole mobilities to majority and minority hole and electron mobilities in compensated p- and n-type silicon. Additionally, we present new mobility data and obtain the parameters from a fit to a larger data base.

Furthermore, we account for the inconsistencies observed in the temperature range from 80 to 350 K. This comprises a new parameterization for hole scattering at phonons and an expression for the temperature dependence of the compensation correction term for majority carrier mobility.

Thus, we present a model for carrier mobilities in silicon which merges with Klaassen's model including a new parameterization for hole scattering at phonons in the case of uncompensated silicon. The data presented in this work suggest that a modification of the electron scattering at phonons would be beneficial as well, which could be considered in a similar way as presented here for hole scattering at phonons. Also, to the best knowledge of the authors no published temperature dependent data of minority carrier mobilities in compensated silicon exists so far. As long as this data is not available, we suggest using the room temperature compensation correction also for modeling the temperature dependence of minority carrier mobilities in compensated silicon.

Acknowledgments

The author would like to thank Michaela Winterhalder and Philipp Barth for sample preparation as well as Achim Kimmerle and Wolfram Kwapil for fruitful discussions.

Appendix A. Mobility data

Table A1 lists the room temperature data of ionized dopant concentrations and majority carrier mobility used for the fit in Section 3.1.1 which has not been published before. Details on the measurements can be found in Refs. [8,9]. The acceptor density N_A has been inferred from Scheil's law from measurements at feedstock level, the donor density N_D has been calculated using N_A and the net doping concentration p_0 from Hall measurements according to $N_D = N_A - p_0$.

Data from the ingots Cz0 (p-type) and Cz0a (n-type) will be part of a separate publication [15], where details on the measurements are explained. For the sake of completeness, they are also listed in Tables A2 and A3.

Table A1
Ionized dopant concentrations and majority hole mobility of samples from mc1, mc2, Cz8, and Cz10.

Sample	T (K)	N_A (cm^{-3})	N_D (cm^{-3})	$\mu_{maj,h}$ ($cm^2\,V^{-1}\,s^{-1}$)
mc1-1	300	9.37×10^{16}	7.66×10^{16}	239
mc1-2	300	8.54×10^{16}	6.01×10^{16}	268
mc1-3	300	8.03×10^{16}	5.23×10^{16}	289
mc1-4	300	7.74×10^{16}	4.58×10^{16}	291
mc1-5	300	7.45×10^{16}	4.38×10^{16}	294
mc1-6	300	7.30×10^{16}	4.14×10^{16}	296
mc2-1	300	9.51×10^{16}	6.35×10^{16}	275
mc2-2	300	9.59×10^{16}	6.70×10^{16}	251
mc2-3	300	9.67×10^{16}	6.67×10^{16}	247
mc2-4	300	1.21×10^{17}	9.58×10^{16}	240
mc2-5	300	1.30×10^{17}	1.06×10^{17}	227
mc2-6	300	1.43×10^{17}	1.18×10^{17}	222
mc2-7	300	1.89×10^{17}	1.64×10^{17}	205
Cz8-1	300	2.64×10^{16}	1.05×10^{16}	356
Cz8-2	300	2.71×10^{16}	1.07×10^{16}	349
Cz8-3	300	2.79×10^{16}	1.17×10^{16}	348
Cz8-4	300	2.89×10^{16}	1.35×10^{16}	350
Cz8-5	300	3.05×10^{16}	1.55×10^{16}	338
Cz8-6	300	3.31×10^{16}	2.18×10^{16}	318
Cz10-1	300	4.14×10^{16}	3.39×10^{16}	281
Cz10-2	300	4.51×10^{16}	3.66×10^{16}	285
Cz10-3	300	5.01×10^{16}	4.16×10^{16}	275
Cz10-4	300	5.64×10^{16}	4.76×10^{16}	254
Cz10-5	300	6.61×10^{16}	5.69×10^{16}	246
Cz10-6	300	8.62×10^{16}	7.51×10^{16}	222
Cz10-7	300	1.32×10^{17}	1.11×10^{17}	197

Table A2
Ionized dopant concentrations and majority hole mobility of samples from ingot Cz0.

Sample	T (K)	N_A (cm^{-3})	N_D (cm^{-3})	$\mu_{maj,h}$ ($cm^2\,V^{-1}\,s^{-1}$)
Cz0-1	295	1.16×10^{16}	5.17×10^{15}	382
Cz0-2	295	1.20×10^{16}	6.01×10^{15}	368
Cz0-3	295	1.25×10^{16}	6.57×10^{15}	368
Cz0-4	295	1.30×10^{16}	8.48×10^{15}	359
Cz0-5	295	1.39×10^{16}	9.85×10^{15}	349
Cz0-6	295	1.56×10^{16}	1.34×10^{16}	308

Table A3
Ionized dopant concentrations and majority electron mobility of samples from ingot Cz0a.

Sample	T (K)	N_A (cm^{-3})	N_D (cm^{-3})	$\mu_{maj,e}$ ($cm^2\,V^{-1}\,s^{-1}$)
Cz0a-1	295	1.17×10^{16}	1.38×10^{16}	832
Cz0a-2	295	1.19×10^{16}	1.44×10^{16}	833
Cz0a-3	295	1.22×10^{16}	1.62×10^{16}	859
Cz0a-4	295	1.37×10^{16}	2.29×10^{16}	863
Cz0a-5	295	1.51×10^{16}	3.17×10^{16}	837
Cz0a-6	295	1.58×10^{16}	3.72×10^{16}	816

Appendix B. Derivation of $\beta_2(T)$

In this section we will explain the origin of the expression for $\beta_2(T)$ from Eq. (11). We observe that for lowly compensated silicon, applying the room temperature correction for compensation with the room temperature compensation level along the whole temperature range delivers very good agreement with experimental data. However, experimental mobility decreases faster than predicted by the room temperature correction the higher the compensation level and the higher the total dopant concentration. Down to a certain reference temperature T_{ref} the room temperature correction works well before the experimental mobility starts to decrease more strongly with decreasing temperature than predicted. We observe that this reference temperature is a function of the total dopant concentration and the compensation level. Fitting the reference temperature plotted as a function of ${C_{l,RT}}^2 \cdot (N_A + N_D)$ delivers the expression from Eq. (12). To account for the stronger decrease starting at the reference temperature T_{ref}, the room temperature compensation level is modified with a function starting to increase for temperatures lower than T_{ref} and corresponding to one for temperatures higher than T_{ref}. This leads to the expression of Eq. (11) in the exponent of the room temperature compensation level. Thus, the compensation level used in the correction term equals the room temperature compensation level for temperatures larger than T_{ref} and increases for temperatures lower than T_{ref} which leads to excellent agreement between model and experimental data.

Appendix C. Model implementation

To facilitate the implementation of the model adaptions to Klaassen's mobility model presented in this work, this section summarizes the crucial points. For modeling carrier mobilities at room temperature, Eq. (5) in [1] has to be replaced by

$$\mu_I = \frac{\mu_N}{((N_I)/(N_{ref,1}))^{\alpha_1} + ((C_{l,RT}-1)/(C_{l,ref}))^{\beta_1}} + \mu_c\left(\frac{c}{N_I}\right) \tag{C.1}$$

for majority carrier mobilities and by

$$\mu_I = \frac{\mu_N}{((N_I)/(N_{ref,1}))^{\alpha_1} + ([(N_A+N_D)/(N_{ref,3})]\cdot[(C_{l,RT}-1)/(C_{l,ref})])^{\beta_1}} + \mu_c\left(\frac{c}{N_I}\right) \tag{C.2}$$

for minority carrier mobilities with the parameters $C_{l,ref}$, β_1, and $N_{ref,3}$ from Section 3.1. This leads to a modification of Eq. (20) in [1] to

$$\mu_{i,D+A+j} = \mu_{i,N}\frac{N_{i,sc}}{N_{i,sc,eff}}\left(\left(\frac{N_{i,sc}}{N_{ref,1}}\right)^{\alpha_1} + \left(\frac{C_{l,RT}-1}{C_{l,ref}}\right)^{\beta_1}\right)^{-1} + \mu_{i,c}\left(\frac{n+p}{N_{i,sc,eff}}\right) \tag{C.3}$$

for majority carriers and to

$$\mu_{i,D+A+j} = \mu_{i,N}\frac{N_{i,sc}}{N_{i,sc,eff}}\left(\left(\frac{N_{i,sc}}{N_{ref,1}}\right)^{\alpha_1} + \left(\left[\frac{N_A+N_D}{N_{ref,3}}\right]\cdot\left[\frac{C_{l,RT}-1}{C_{l,ref}}\right]\right)^{\beta_1}\right)^{-1} + \mu_{i,c}\left(\frac{n+p}{N_{i,sc,eff}}\right) \tag{C.4}$$

for minority carriers.

To correctly account for the temperature dependence, the expression for the lattice scattering mobility in Eq. (1) in [14] should be replaced by Eq. (7) of this work for holes. To additionally include the temperature dependence of the majority carrier mobility due to scattering at ionized impurities accounting for

compensation, Eq. (C.3) converts to

$$\mu_{i,D+A+j} = \mu_{i,N}\frac{N_{i,sc}}{N_{i,sc,eff}}\left(\left(\frac{N_{i,sc}}{N_{ref,1}}\right)^{\alpha_1}/\left(\frac{T}{300\ \mathrm{K}}\right)^{3\alpha_1-1.5} + \left(\frac{C_{l,RT}{}^{\beta_2(T)}-1}{C_{l,ref}}\right)^{\beta_1}\right)^{-1} + \mu_{i,c}\left(\frac{n+p}{N_{i,sc,eff}}\right)\left(\frac{300\ \mathrm{K}}{T}\right)^{0.5} \quad (C.5)$$

Note that in this formulation, $\mu_{i,N}$ and $\mu_{i,c}$ are the temperature independent expressions from Eqs. (3b) and (3c) in reference [1] and $\beta_2(T)$ is the temperature dependent term from Eq. (11) of this work. As there is no data for temperature dependent minority carrier mobilities in compensated silicon, $\beta_2(T)$ could not be adjusted for minority carriers. As long as there is no data available, we suggest to use the following expression for modeling temperature dependent minority carrier mobilities:

$$\mu_{i,D+A+j} = \mu_{i,N}\frac{N_{i,sc}}{N_{i,sc,eff}}\left(\left(\frac{N_{i,sc}}{N_{ref,1}}\right)^{\alpha_1}/\left(\frac{T}{300\ \mathrm{K}}\right)^{3\alpha_1-1.5} + \left(\left[\frac{N_A+N_D}{N_{ref,3}}\right]\cdot\left[\frac{C_{l,RT}-1}{C_{l,ref}}\right]\right)^{\beta_1}\right)^{-1} + \mu_{i,c}\left(\frac{n+p}{N_{i,sc,eff}}\right)\left(\frac{300\ \mathrm{K}}{T}\right)^{0.5} \quad (C.6)$$

which includes the room temperature compensation correction term over the whole temperature range. As shown in Fig. 4 for majority carrier mobilities, this would probably overestimate the mobility for highly compensated silicon at low temperatures. Still, this error will be smaller over the whole temperature range than modeling without any compensation correction.

References

[1] D.B.M. Klaassen, A unified mobility model for device simulation – I. Model equations and concentration dependence, Solid-State Electron. 35 (1992) 953–959.

[2] J. Libal, S. Novaglia, M. Acciarri, R. Petres, J. Arumughan, R. Kopecek, A. Prokopenko, Effect of compensation and of metallic impurities on the electrical properties of Cz-grown solar grade silicon, J. Appl. Phys. 104 (2008) 104507.

[3] F. Schindler, J. Geilker, W. Kwapil, J.A. Giesecke, M.C. Schubert, W. Warta, Conductivity mobility and Hall mobility in Compensated multicrystalline silicon, in: Proceedings of the 25th European Photovoltaic Solar Energy Conference, Valencia, Spain, 2010, pp. 2364–2368.

[4] J. Veirman, S. Dubois, N. Enjalbert, J.P. Garandet, D.R. Heslinga, M. Lemiti, Hall mobility reduction in single-crystalline silicon gradually compensated by thermal donors activation, Solid-State Electron. 54 (2010) 671.

[5] M. Forster, E. Fourmond, R. Einhaus, H. Lauvray, J. Kraiem, M. Lemiti, Ga co-doping in Cz-grown silicon ingots to overcome limitations of B and P compensated silicon feedstock for PV applications, Phys. Status Solidi (c) 8 (2011) 678–681.

[6] E. Fourmond, M. Forster, R. Einhaus, H. Lauvray, J. Kraiem, M. Lemiti, Electrical properties of boron, phosphorus and gallium co-doped silicon, Energy Procedia 8 (2011) 349–354.

[7] B. Lim, M. Wolf, J. Schmidt, Carrier mobilities in multicrystalline silicon wafers made from UMG-Si, Phys. Status Solidi C 8 (2011) 835–838.

[8] M. Forster, A. Cuevas, E. Fourmond, F.E. Rougieux, M. Lemiti, Impact of incomplete ionization of dopants on the electrical properties of compensated p-type silicon, J. Appl. Phys. 111 (2012) 043701–043707.

[9] M. Forster, Compensation engineering for silicon solar cells (Ph.D. thesis), National Institute for Applied Sciences (Lyon) and The Australian National University, 2012.

[10] F. Schindler, M.C. Schubert, A. Kimmerle, J. Broisch, S. Rein, W. Kwapil, W. Warta, Modeling majority carrier mobility in compensated crystalline silicon for solar cells, Sol. Energy Mater. Sol. Cells 106 (2012) 31–36.

[11] M. Forster, F.E. Rougieux, A. Cuevas, B. Dehestru, A. Thomas, E. Fourmond, M. Lemiti, Incomplete ionization and carrier mobility in compensated p-type and n-type silicon, IEEE J. Photovolt. 3 (2013) 108–113.

[12] J. Veirman, B. Martel, S. Dubois, J. Stendera, Effect of dopant compensation on the temperature dependence of the transport properties in p-type monocrystalline silicon, J. Appl. Phys. 115 (2014) 083703.

[13] D.M. Caughey, R.E. Thomas, Carrier mobilities in silicon empirically related to doping and field, Proc. IEEE 55 (1967) 2192–2193.

[14] D.B.M. Klaassen, A unified mobility model for device simulation – II. Temperature dependence of carrier mobility and lifetime, Solid State Electron. 35 (1992) 961–967.

[15] J. Broisch, F. Schindler, M.C. Schubert, A.-K. Soiland, F. Fertig, S. Rein, Resistivity, doping concentrations and carrier mobilities in compensated n- and p-type Czochralski silicon: comparison of measurements and simulations and consistent description of material parameters, to be published (2014).

[16] F. Schindler, J. Geilker, W. Kwapil, W. Warta, M.C. Schubert, Hall mobility in multicrystalline silicon, J. Appl. Phys. 110 (2011) 043722.

[17] F. Szmulowicz, Acoustic and optical-phonon-limited mobilities in p-type silicon within the deformation-potential theory, Appl. Phys. Lett. 43 (1983) 485–487.

[18] W.C. Mitchel, P.M. Hemenger, Temperature dependence of the Hall factor and the conductivity mobility in p-type silicon, J. Appl. Phys. 53 (1982) 6880–6884.

[19] F. Szmulowicz, Calculation of the mobility and the Hall factor for doped p-type silicon, Phys. Rev. B 34 (1986) 4031–4047.